Atmospheric
Chemistry
and Physics

Open Access

Discussions

Diurnal variations of stratospheric ozone measured by ground-based microwave remote sensing at the Mauna Loa NDACC site: measurement validation and GEOSCCM model comparison

A. Parrish[1], I. S. Boyd[2], G. E. Nedoluha[3], P. K. Bhartia[4], S. M. Frith[5], N. A. Kramarova[5], B. J. Connor[6], G. E. Bodeker[7], L. Froidevaux[8], M. Shiotani[9], and T. Sakazaki[9]

[1]Department of Astronomy, University of Massachusetts, Amherst, MA, USA
[2]Contractor to BC Scientific Consulting LLC, USA
[3]Naval Research Laboratory, Washington, DC, USA
[4]NASA-Goddard Space Flight Center, Greenbelt, MD, USA
[5]SSAI, Lanham, MD, USA
[6]BC Scientific Consulting LLC, Wellington, New Zealand
[7]Bodeker Scientific, Alexandra, New Zealand
[8]Jet Propulsion Laboratory, Pasadena, CA, USA

[9]Research Institute for Sustainable Humanosphere, Kyoto University, Uji, Japan

Correspondence to: A. Parrish (parrish@astro.umass.edu) and
I. S. Boyd (iboyd@astro.umass.edu)

Measurement validation and GEOSCCM model comparison

A. Parrish et al.

Title Page

Abstract | Introduction

Conclusions | References

Tables | Figures

|◄ | ►|

◄ | ►

Back | Close

Full Screen / Esc

Printer-friendly Version

Interactive Discussion

Abstract

There is presently renewed interest in diurnal variations of stratospheric and mesospheric ozone for the purpose of supporting homogenization of records of various ozone measurements that are limited by the technique employed to being made at certain times of day. We have made such measurements for 18 yr using a passive microwave remote sensing technique at the Mauna Loa Observatory in Hawaii, which is a primary station in the Network for Detection of Atmospheric Composition Change (NDACC). We have recently reprocessed these data with hourly time resolution to study diurnal variations. We inspected differences between pairs of the ozone spectra (e.g. day and night) from which the ozone profiles are derived to determine the extent to which they may be contaminated by diurnally varying systematic instrumental or measurement effects. These are small, and we have reduced them further by selecting data that meet certain criteria that we established. We have calculated differences between profiles measured at different times: morning–night, afternoon–night, and morning–afternoon and have intercompared these with like profiles derived from Aura-MLS, UARS-MLS, SMILES, and SBUV/2 measurements. Differences between averages of coincident profiles are typically < 1.5 % of typical nightime values over most of the covered altitude range with some exceptions. We calculated averages of ozone values for each hour from the Mauna Loa microwave data, and normalized these to the average for the first hour after midnight for comparison with corresponding values calculated with the Goddard Earth Observing System Chemistry Climate Model (GEOSCCM). We found that the measurements and model output mostly agree to better than 1.5 % of the midnight value, with one noteworthy exception: the measured morning–night values are significantly (2–3 %) higher than the modeled ones from 3.2 to 1.8 hPa ($\sim$ 39–43 km), and there is evidence that the measured values are increasing compared to the modeled values before sunrise in this region.

1 Introduction

Chapman (1930) first described a theory that, although it included only five reactions between various oxygen species and did not consider dynamics, predicted several of the major features of the stratospheric ozone layer. The reactions include the formation of the precursors of ozone by photodissociation of molecular oxygen, and also ozone,

$$O_3 + h\nu \rightarrow O + O_2 \qquad\qquad (R1a)$$

and

$$O_3 + h\nu \rightarrow O(1D) + O_2. \qquad\qquad (R1b)$$

The latter products re-form ozone via the reaction

$$O_2 + O + M \rightarrow O_3 + M, \qquad\qquad (R2)$$

where M is a third, non-reacting atom or molecule that must be simultaneously involved with the oxygen species to carry away the energy liberated in the reaction. The solar energy absorbed in this cycle is the main source of heating in the stratosphere and contributes strongly to the observed increase in atmospheric temperature with altitude in this region. Branch (R1b) of the ozone photodissociation reaction absorbs strongly at wavelengths < 310 nm, and filters out the biologically damaging solar UVB radiation (280 to 320 nm) that would otherwise reach the Earth's surface. This science was of little interest to international policymakers until the realization that ozone could also be destroyed globally in a catalytic cycle by chlorine initially released in the upper stratosphere by photodissociation of human-made chlorofluorocarbons (Rowland and Molina, 1975). This, and the later discovery of the Antarctic ozone "hole" (Farman et al., 1985), led to much more intensive study of the upper atmosphere through measurements of the relevant oxygen, hydrogen, nitrogen, chlorine and bromine species, laboratory measurements of their reaction rates, and computational modeling of the chemistry and dynamics of the stratosphere using these data. These efforts convinced

policymakers to enact the Montreal Protocol (UNEP, 2006). As a result of this international treaty, the level of ozone depleting substances (ODS) peaked in 1996 and has since been declining (WMO, 2011). This assessment concluded that the ozone decline from ∼ 1980 to the mid-1990s ceased around 1996. It also noted that while the trend values seen from 1996–2008 were positive and consistent with expected ozone recovery, they were not statistically significant. Further refinement of ozone records will reduce the time required to make the latter detection with a high degree of confidence.

The effort to determine the long-term behavior of stratospheric ozone profiles has relied upon measurements made with a variety of satellite and ground-based instruments employing various physical techniques. No single individual instrument has produced a highly stable, global record of ozone profiles over the entire period of interest. The longest such record to date was produced from 1984 to 2005 by the Stratospheric Aerosol and Gas Experiment (SAGE-II) instrument. Past analyses, e.g. SPARC (1998), relied heavily on the SAGE-II data set. A complete record from, say, the 1980s to the present must therefore be assembled from multiple shorter records. This requires evaluating effects of, e.g. systematic measurement drift due to instrument degradation and calibration offsets between individual instruments or instrument types on the assembled record. In addition to these measurement issues, real diurnal ozone variations must be accounted for when combining records from instruments that make measurements at different times of day. For example, SAGE-II made measurements only at sunrise and sunset. There are also diurnal issues with data from the several Solar Backscatter Ultraviolet (SBUV, SBUV/2) instruments because the orbits of most of their carrier satellites drifted in such a manner that the times of their measurements over a given location changed by several hours over the course of a few years. Thus, an accurate understanding of diurnal ozone variations facilitates the effort of combining these and other measurements into an accurate and homogeneous long-term climate data record for ozone.

The fact that the reactions listed above and many others in the contemporary understanding of upper atmospheric chemistry involve photodissociation implies that diurnal

Measurement validation and GEOSCCM model comparison

A. Parrish et al.

Title Page

Abstract | Introduction

Conclusions | References

Tables | Figures

|◄ | ►|

◄ | ►

Back | Close

Full Screen / Esc

Printer-friendly Version

Interactive Discussion

variations will occur as long as the reaction time constants are $\ll 24$ h. To take a simple example, because Reaction (R2) requires the simultaneous presence of three species to occur, its rate is proportional to the square of the density. Thus, in the mesosphere, where the density is very low, Reaction (R2) occurs much less rapidly than Reaction (R1), and nearly all of the odd oxygen $(O + O_3)$ is in atomic form during the day but quickly forms ozone through Reaction (R2) at sunset. As figures in this and earlier papers, e.g. Connor et al. (1994) show, daytime ozone mixing ratios in the mesosphere are $\sim 70\%$ less than nighttime reference values at 0.1 hPa. As altitude decreases and pressure increases the diurnal variations quickly become smaller. Between 1 and 5 hPa they are small enough that they attracted little attention until Huang et al. (1997) analyzed UARS-MLS data and claimed detection of an afternoon ozone enhancement (when compared to evening and morning values) of several percent at 3 hPa. There were concerns about this result because the same analysis showed unexpectedly large diurnal variations at lower levels, e.g. 10 hPa. However, ground-based microwave measurements by Haefele et al. (2008) also showed an afternoon enhancement at ~ 3 hPa. In any case, these small variations are important when homogenizing multiple ozone records because the upper stratospheric ozone depletion reaches its maximum in this region.

Diurnal measurements are made most conveniently with a space- or ground-based spectroscopic instrument that measures a thermally excited ozone emission line at microwave or infrared wavelengths. Infrared measurements may be subject to errors if the transition involved is not in local thermodynamic equilibrium, as noted by Connor et al. (1994). This is not an issue for transitions in the microwave region because there the energy levels are more closely spaced. Ground-based emission measurements can be made over the full 24 h, weather permitting, with negligible contamination from other ozone anomalies, but the measurements are limited to the few locations where such instruments are sited. Satellite-based measurements typically cover a wide range of latitudes, but have limitations arising from the nature of their orbits. For example, the Aura satellite carrying the second JPL Microwave Limb Sounder (hereafter Aura-MLS)

is in a sun-synchronous orbit, so it passes over a given location only twice per day. The orbit of the UARS satellite carrying the first MLS (hereafter UARS-MLS) precessed such that it cycled through 24 h over a given location once every ∼ 36 days, which allowed complete diurnal sampling. Likewise, the orbit of the International Space Station carrying the Superconducting Submillimeter-Wave Limb-Emission Sounder (hereafter SMILES) cycled through 24 h every 60 days, enabling the diurnal observations reported by Sakazaki et al. (2013). In such cases, seasonal ozone variations must be accounted for when comparing a measurement at one time of day with that from another, as the latter may have been taken several tens of days later or earlier, depending on the rate of precession of the satellite orbit. There have been several approaches to this problem. For example, Huang et al. (1997, 2010) separated the diurnal and seasonal components in UARS-MLS data by making Fourier series of these two components out of time series of the data. Sakazaki et al. (2013) extracted the diurnal variations from the SMILES data by subtracting a 30 day running mean of the time series from the original data. These two approaches gave quite different results, particularly in the lower stratosphere. The amplitude of the equatorial diurnal variations derived from UARS-MLS data shown in Fig. 6 in Huang et al. (2010) at 32 hPa (∼ 24 km) are 5 to 10 % of the midnight value, while they are ≤ 0.05 ppm (∼ 2 %) in Fig. 5 in Sakazaki et al. (2013). These differences could be due either to the analysis technique or to real differences between the two data sets. The first possibility can be avoided by comparing only measurements made at specific times of day, as we do in this paper, but these are limited to the available satellite overpass times.

Models could also be used to determine diurnal adjustments when homogenizing multiple data sets, provided they adequately represent the complex chemical and dynamical phenomena in the atmosphere. Recent comparisons of SMILES data with two chemical climate models (Sakazaki et al., 2013) show good agreement, suggesting that current models may be sufficiently sophisticated to use for data set homogenization. To contribute to this study, we compare measurements made with the ground-based

Title Page

Abstract | Introduction

Conclusions | References

Tables | Figures

|◄ | ►|

◄ | ►

Back | Close

Full Screen / Esc

Printer-friendly Version

Interactive Discussion

NDACC microwave ozone profiling radiometer (MWR) at Mauna Loa, Hawaii (19.5° N, 204.5° E) with available output from the NASA-GEOSCCM model in this paper.

The remainder of this paper is organized as follows: Sect. 2 discusses the MWR measurements and the selection of data that we found necessary to minimize small in-
5 strumental effects on the results. Section 3 compares the MWR measurements to those made with the satellite-borne Aura-MLS, UARS-MLS, SMILES, and several SBUV/2 instruments to establish the degree of agreement between these resources and the quality of the MWR data. Technical references for these instruments are also given in this section. Section 4 discusses the model-measurement comparison. Section 5
10 summarizes the work.

2 Ground-based microwave measurements

The Mauna Loa MWR has been in operation since 1995. The instrument consists of a heterodyne receiver coupled to a 120 channel filter spectrometer. It measures the emission spectrum of a line produced by a thermally excited, purely rotational ozone
15 transition at 110.836 GHz (2.7 mm wavelength). The spectral intensities and measurements of the tropospheric thermal emission are calibrated with black body sources at ambient and liquid nitrogen temperatures. The tropospheric opacity is calculated from hourly emission measurements. The experimental technique was described in Parrish et al. (1992), and technical details on the instrument used for this work are given in
20 Parrish (1994).

One technical point that is pertinent to the discussion that follows is that the instrument was designed so that the elevation angle of the primary signal beam (the line of sight through the atmosphere) is automatically adjusted to compensate for weather-induced variations in the tropospheric opacity. The compensation technique and the
25 need for it are discussed in Parrish et al. (1988). The elevation angle increases approximately linearly with the tropospheric opacity. The peak of the distribution of the number of observations as a function of the elevation angle at which they were made is

Title Page

Abstract | Introduction

Conclusions | References

Tables | Figures

◄ | ►►

◄ | ►

Back | Close

Full Screen / Esc

Printer-friendly Version

Interactive Discussion

at 12.5°. The instrument typically operates at or within a few degrees above this value when the weather is clear or clouds are thin. As the weather degrades, the elevation angle increases and the distribution decreases smoothly from its peak. The number of measurements made at elevation angles above $\sim 24°$ is negligible. When the weather is exceptionally good, the distribution drops off quickly from its peak to zero at $\sim 10°$.

The ozone mixing ratio profiles are retrieved from the spectra using an adaptation of the optimal estimation method of Rodgers (1976), discussed in Parrish et al. (1992) and Connor et al. (1995). Our error analysis techniques are discussed in the latter paper. The independent variable in the retrieval system is pressure; we give approximate corresponding altitudes in the text and figures in some instances for convenience. We define the vertical resolution of the measurements as the full width to half maximum of the typical averaging kernels. The derivation of the averaging kernels and the resolution are described in Connor et al. (1995). The kernel half width has a minimum of 6 km at an altitude of 32 km, lies between 6 and 8 km between 20 and 42 km, and then increases to 14 km at 65 km. These values are slightly smaller than those described in Connor et al. (1995) due to procedural improvements and retrieval parameter readjustments which are applicable to the present version 6 of the MWR data.

We reprocessed the MLO 1995 to 2013 MWR data with hourly time resolution for use in this work. While this resolution is not adequate for studying the rapid ozone transitions in the mesosphere at sunrise and sunset, it suffices to observe slower diurnal variations at other times of day. The processing procedures for these data are the same as those for the standard MLO MWR product that is submitted to the NDACC database. The hourly data are not included in the submission, but are available from the corresponding author upon request.

2.1 A note on units

Data and plots presented in this paper have been normalized to reference values, and results have been expressed in percent, i.e., Percent = $100.0 \times (VMR_{DATA} - VMR_{REF})/VMR_{REF}$, where VMR_{DATA} are the data being normalized, in units of volume

mixing ratio, and VMR$_{REF}$ are the pressure-corresponding reference data. The original data from all instruments except SMILES were provided in units of volume mixing ratio (VMR) vs. pressure. The SMILES data were converted as described in Sect. 3. Unless otherwise noted, the reference data were taken at night. The times at which the reference data were taken are noted in the text or in the figures. In the following comparisons between two profiles taken under different conditions or with different instruments, quoted values represent the differences between pressure-corresponding data points in the profiles. While these are absolute differences, they are expressed in percent because the profiles being compared are given in units of percent.

2.2 Study and mitigation of diurnally varying errors in the microwave measurements

We found that the measurements were being affected by diurnal temperature variations within the small outbuilding (hereafter referred to as "room") housing the instrument. While the temperatures we theoretically need to process the raw data are automatically measured, recorded and utilized in the analysis, there appear to be small secondary temperature effects on the measurements. The largest room temperature changes occurred on cold and windy nights when there was not enough heat available to keep the room temperature at the thermostat setting. The temperature would also occasionally rise above this setting during the warmest sunny days. About three-quarters of all measurements between 2004 and 2012 were made with the room temperature controlled by the thermostat, which is typically set to 20 °C.

We compared day-night difference profiles made up from data taken at temperatures within ±1.2 °C of the thermostat setting to data taken at all room temperatures, and the results are shown in Fig. 1. This figure shows the percentage differences vs. pressure between our daytime (early afternoon, 12:36 to 13:36 local solar time, 23:00 to 24:00 UTC) and nighttime (01:36 to 02:36 LST, 12:00 to 13:00 UTC) measurements averaged over the period August 2004 to March 2013. The day- and night-times used were those of the Aura-MLS overpasses so that this figure is comparable to others

shown later. The violet line shows the result obtained if we use data processed with the standard quality selection criteria that are applied to MWR data submitted to the NDACC database, hereafter designated "standard" data. The red line shows the result obtained if we select data meeting the temperature criteria described above in addition to the standard criteria. They are designated hereafter as "temperature controlled" data in the text and figure captions. These two profiles have apparent local minima at ~ 24 and ~ 37 km and a local maximum at ~ 32 km. The maximum and minima are effects of the retrieval process in combination with residual systematic errors in the spectra. The retrieval tends to alternately overestimate and underestimate (or vice versa) the ozone values as altitude increases, and systematic spectral errors drive up the amplitude of these variations, as discussed below. The amplitude of these variations is reduced by a factor of about 2 when the data are controlled for temperature. Another feature in Fig. 1 is that the values in the temperature controlled profile are up to ~ 1 % larger than the corresponding values in the standard profile. This could be an effect of selecting out the tropospheric conditions that produce the windy weather, or a presently unknown, temperature-dependent instrumental calibration error. In either case, we believe that reducing the range of diurnal temperature variations should lead to improved accuracy in the diurnal difference profile measurements, and therefore use only temperature controlled data for the work presented below.

We also found that details in our diurnal difference profiles depended on the range of signal beam elevation angles (discussed in Sect. 2.0) over which they were taken. Figure 2 gives several examples that display maxima and minima similar to those shown in Fig. 1. The red profile corresponds to the red profile in Fig. 1. The others show results obtained if we select measurements that meet the temperature criteria and also were made within the indicated ranges of signal beam elevation angles. These lines have very nearly the same pattern as the red line except that the magnitudes of the minima and maxima are increased if the lower (11.5° to 12.5°) elevation angle range is used (green) and nearly eliminated if only data taken at elevation angles > 13.5° are used (black). We chose the angles for the former profile to force a worst-case condition

and clearly demonstrate the maxima and minima. The blue profile shows the effect of restricting elevation angles to > 14.5°. In this case, the small local maxima reappear where the minima are on the other profiles, and vice versa. We argue below that the data selection leading to the black profile is optimum for this work.

2.2.1 Systematic error tests using spectral differences

We inspected day (designated D) minus night (designated N) difference spectra to see what effect the beam elevation angle range had on the differential systematic spectral errors. The fact that the true spectrum of an ozone line is symmetric about its center provides a means for detecting artifacts in a measured spectrum. Other features in the difference spectra are systematic artifacts. They will introduce errors in the corresponding retrieved difference profiles unless they are perfectly antisymmetric about the ozone line center, which is unlikely. The intensities of the ozone signals seen in the individual D and N spectra depend on the signal beam elevation angle θ and zenith tropospheric opacity τ_z at the times the observations were made, and these parameters may differ from one observation to another. Their intensity scales are therefore renormalized to account for θ and τ_z at the times that the D and N measurements were made. The spectra were scaled as if the observations were made at the long term average values of θ and τ_z (14.1° and 0.09 nepers, respectively). All but the small differences between spectra D and N then cancel out when the second is subtracted from the first. We then prepared averages of these D-N spectra over extended periods of time to reduce the noise. Those in Fig. 3 were averaged over the same period and times of day as the corresponding profiles presented in Fig. 2. The differenced ozone line is the central feature in the spectrum. The intensity of this feature cannot be intuitively interpreted because θ is not constant and the atmosphere is not plane parallel. The large negative feature at the center of the spectrum is due to the reduced values of daytime ozone relative to those at nighttime in the upper stratosphere and mesosphere. It is shown with an expanded frequency scale in the bottom panel of Fig. 3. It is very narrow because the spectral pressure broadening is small, given the low atmospheric pressure in this

Title Page

Abstract | Introduction

Conclusions | References

Tables | Figures

|◀ | ▶|

◀ | ▶

Back | Close

Full Screen / Esc

Printer-friendly Version

Interactive Discussion

region. The surrounding symmetric positive features seen in the top panel of the figure are due to enhanced daytime ozone in the region of 1 to 10 hPa.

The quasi-sinusoidal feature seen most prominently on the left side of the green spectrum in Fig. 3 is an asymmetric artifact. This curve corresponds to the forced worst-case green profile in Fig. 2. Such features are commonly seen in spectra produced by instruments like the MWR due to the presence of an unintended interferometer in the signal path between the sky and the input to the receiver electronics, caused by weak reflections at devices in this path. The red spectrum is obtained when no restrictions are placed on the elevation angle. It contains a weak artifact like that seen in the green spectrum. It is smaller still in the black spectrum. The blue spectrum shows that the phase of the quasi-sinusoidal feature is substantially changed if the minimum elevation angle is raised to 14.5°. Such phase shift occurs when the spacing between the reflecting devices in an interferometer is changed, and is reasonable given the system window configuration, which is shown in Parrish (1994).

We believe that the best estimate of the day-night MWR difference profiles is obtained by selecting data that are taken both at a room temperature within ±1.2 °C of the thermostat setting and at elevation angles > 13.5° because the temperature constraint minimizes the potential impact of diurnal room temperature variations on the measurements, and the angle constraint minimizes both the known artifacts in the difference spectrum shown for that angle range in Fig. 3 and the maxima and minima in the corresponding difference profile in Fig. 2. We use data selected in this manner for the work presented in the remainder of this paper.

3 Comparison of MWR and satellite measurements

We have compared difference profiles (e.g. day-night) derived from the MWR data with those derived from several satellite-borne instruments to evaluate the consistency of these data sources. The satellite instruments are: Aura-MLS (Waters et al., 2006; Froidevaux et al., 2008), UARS-MLS (Barath et al., 1993; Froidevaux et al., 1996;

Discussion Paper | Discussion Paper | Discussion Paper | Discussion Paper | Discussion Paper |

Livesey et al., 2003), three Solar Backscatter Ultraviolet (SBUV/2) instruments aboard NOAA operational satellites (Frederick et al., 1986), and SMILES (Kikuchi et al., 2010).

Figure 4 compares daytime minus nighttime profiles measured with the MWR with those measured with Aura-MLS. This instrument measures the emission spectrum of a rotational transition of ozone at 243.6 GHz. We obtained the version 3.3 data from the Goddard Earth Sciences Data and Information Services Center (hereafter GES DISC); they are described in Livesey et al. (2011). Aura is in a sun-synchronous orbit; we use measurements made when it passes over MLO (early afternoon, 12:36 to 13:36 LST; night 01:36 to 02:36 LST). We calculated individual difference profiles for each day when there was a daytime profile and a nighttime profile within 15 h of each other, and within 1° latitude and 6° longitude of MLO. These profiles were averaged for the indicated seasons from the beginning of Aura-MLS measurements in August 2004 through March 2013. The MWR profiles plotted in black were generated from MWR data that were selected as described previously, taken within a half hour of the MLS day and night overpass times, and were within 15 h of each other. There were 127 such measurement pairs in summer, 119 in autumn, 120 in winter, and 104 in spring. We did not select an Aura-MLS pair that matched each MWR pair in time. The number of Aura measurements per unit time varies negligibly during the comparison period and there are no substantial gaps in the MWR measurements, so it is unlikely that a selection effect is introduced in the absence of any control on the difference in dates between the Aura-MLS and MWR measurements. The Aura-MLS data (red) were convolved with the MWR averaging kernels as described in Connor et al. (1995) to make them directly comparable in terms of vertical resolution. The differences between the original and convolved Aura-MLS data are typically < 1 % below 1 hPa (∼ 48 km). Above this level, some differences are larger than the two standard deviation statistical error bars. We have included the dashed blue profiles derived directly from original Aura-MLS data in Fig. 4 to demonstrate these effects.

Differences between the MWR and Aura-MLS profiles in Fig. 4 are < 0.7 % between 30 and 3 hPa (∼ 24 and 40 km) when averaged over all seasons. Below and above

CC BY

these levels the Aura-MLS values increase with respect to the MWR values. The differences reach $\sim 1\%$ at 56 and 2 hPa (~ 20 and 43 km) on average. Because their maximum differences do not consistently occur at a particular altitude, they will tend to be smoothed out in an all-season average. The largest bias, $\sim 3\%$, is seen in winter between 1.3 and 0.8 hPa (~ 46 and 50 km). This apparent bias may be partially due to statistical fluctuations. Around 0.6 hPa (~ 52 km) both the Aura-MLS and MWR profiles show a progression of decreasing day-night ozone differences from summer though winter, with recovery in the spring.

The Aura-MLS day-night profiles in Fig. 4 vary little with season, $< 1\%$, below 1 hPa. The MWR profiles vary more, lie above the Aura-MLS profiles at some altitudes but below at others, and the pattern differs from season to season. This pattern in the MWR profiles may superficially appear to be similar to the patterns in MWR profiles affected by systematic errors shown in Fig. 2. However, the major component of the fluctuations in the Fig. 4 profiles is statistical in nature. We determined this by extending the beginning of the averaging period back to August 1995 to substantially increase the number of profiles in the averages (not shown). In this case there were 232 individual profiles in the average for summer, 96 for autumn, 195 for winter, and 266 for spring. As expected for statistical fluctuations, we found that amplitude of the profile fluctuations decreased, going approximately as the inverse square root of the number of profiles contained in the averages, when compared to the averages shown in Fig. 4.

We compared day-night measurements made with the SMILES, Aura-MLS, and MWR instruments. SMILES began operating on 12 October 2009 and failed on 21 April 2010. Its profiles are derived from spectral measurements of a rotational transition of ozone at 625.4 GHz. Its ozone measurements were made in either of two receiver configurations, known as "Band A" and "Band B"; these are described in Kikuchi et al. (2010). We excluded from the average difference profiles described below individual profiles in which the daytime measurement was made with the instrument set up in Band A while the nighttime measurement was made in Band B or vice versa; this was done to eliminate potential systematic effects that could otherwise appear. Valida-

tion of SMILES ozone data is described in Imai et al. (2013). The native units of the SMILES L2 version 2.1 data are mixing ratio vs. altitude. In this comparison, we use pressures supplied with the data for conversion to the mixing ratio vs. pressure native units of Aura-MLS and MWR. The pressure values included with the SMILES data are derived, assuming hydrostatic equilibrium, from atmospheric temperature profiles also measured by SMILES (JAXA, 2012). The instrument overpasses MLO twice each day, cycling through 24 h every ∼ 60 days. It is therefore possible to obtain profile differences between pairs of times separated by roughly 12 h, although at some times of day there are very few measurements. For the time ranges 11:36 to 15:36 and 23:36 to 03:36 LST at Mauna Loa, there were six groups of SMILES day-night measurement pairs, approximately equally spaced between October 2009 and March 2010. The minimum number of pairs was 4 per group, the maximum 14, and the average 8. The time ranges were chosen to maximize the number of SMILES pairs included in the average while also including the Aura-MLS overpass times. Figure 5 displays the day-night difference profiles derived from these measurement pairs, and likewise the Aura-MLS and MWR profiles. The MWR and Aura-MLS profiles were also averaged over the time and date ranges indicated above.

The day-night profiles shown in Fig. 5 from the three instruments agree within 1.5 % from 56 to 0.4 hPa (∼ 20–54 km). In this range, the differences between seventy-seven percent of the total number of MWR and Aura-MLS pressure-corresponding data point pairs are < 1 %, as defined in Sect. 2.1. Likewise, seventy-seven percent of the MWR-SMILES differences and fifty-five percent of the AURA-MLS – SMILES differences are < 1 %. Further, all of the individual profiles lie within 1 % of the average of the three profiles up to 0.7 hPa (∼ 50 km). The MWR profile mostly lies between the SMILES and Aura-MLS profiles, so the difference between the MWR profile and the average of the SMILES and Aura-MLS profiles is < 1 % from 56 to 0.3 hPa (∼ 20 to 56 km). All three profiles peak at ∼ 2.5 % between 5 and 3 hPa (35 and 40 km.). Above 0.4 hPa (∼ 54 km), the differences between Aura-MLS and the other two instruments are 2 % or more, with the Aura-MLS values less negative, as in Fig. 4. The MWR minus Aura-

MLS differences are smaller than they are in the winter panel of Fig. 4, because they are being averaged over all seasons. They are statistically significant only at 0.2 hPa (~ 58 km).

There are small differences between Figs. 4 and 5 above 3 hPa (~ 40 km). These may result from a selection effect given the fact that the SMILES and MWR profiles in Fig. 5 were averaged over four hour time blocks while the Aura-MLS measurements lie within one hour blocks. We attempted to test for such an effect by calculating a MWR profile (not shown in the figure) where the data were averaged over just one hour centered on the MLS overpass times. The precision of this test was poor because the MWR profile is made up from only 15 measurement pairs. Nonetheless, this profile lies within 2.5 % of the MWR and Aura-MLS profiles in Fig. 5, and the differences are not statistically significant.

In Fig. 6 we show comparisons for another time period, morning–night, using data from UARS-MLS, MWR, and SMILES. UARS-MLS profiles are derived from the spectra of a rotational ozone transition at 206.13 GHz. The data were obtained from GES DISC and are described in Livesey et al. (2003). To optimize the number of morning measurements we used data between 07:36 to 10:36 LST for morning and 21:36 to 00:36 LST for night, for all instruments. Coincidence in time between the satellite and MWR measurements is unfortunately an issue. UARS-MLS passed over MLO at varying times, but made very few morning measurements after the MWR began operating in 1995; most of the UARS-MLS measurements were made in the September 1991 to May 1994 period, while the MWR data are from July 1995 up to January 1998. The latter date was chosen to correspond to the date when UARS-MLS measurements ended. The MWR was operating throughout the period when SMILES was making measurements. There are six groups of SMILES difference profiles during this period, with a total of 27 profiles. The figure shows a second MWR profile that covers the period 19 October 2009 to 20 April 2010 to cover the period of measurements included in the SMILES profile.

Title Page

Abstract | Introduction

Conclusions | References

Tables | Figures

|◄ | ►|

◄ | ►

Back | Close

Full Screen / Esc

Printer-friendly Version

Interactive Discussion

All four profiles in Fig. 6 have similar shapes and these are noticeably different than the profiles in Fig. 5. In Fig. 6 the values are positive between about 3 and 1.3 hPa ($\sim$ 40 to 46 km), while in Fig. 5 the values are positive between about 10 and 2 hPa ($\sim$ 32 to 43 km). However, the differences between profiles are larger than they are in Fig. 5. We compared the satellite (UARS-MLS or SMILES) values and their corresponding MWR values, and found that only forty percent of the total number of differences between pressure-corresponding data points are within 1 % of each other. Seventy percent are within 1.5 %, and ninety percent are within 2 %, and all are within 2.1 %. Even though the SMILES data were taken $\sim$ 15 yr later than the UARS-MLS data, agreement of the day-night profile values for this pair is similar to those just described. Thirty-five percent of the differences are within 1 %, 65 % are within 2 %, and all are within 2.7 %. The August 1995 to January 1998 MWR profile corresponding to the UARS-MLS profile is alternately lower and higher than the latter up to 1.8 hPa ($\sim$ 43 km). The character of these fluctuations is similar to those shown in Fig. 2. Possibly there is a systematic contribution of the order of 1 % to the profile during this early period that is not yet understood. These fluctuations therefore should not be regarded as reliable pending further investigation.

In Fig. 7, we have constructed difference profiles from the measurements of pairs of SBUV/2 instruments on NOAA operational satellites that pass over MLO at different times of the day. We derived the SBUV/2 profiles from the March 2013 reprocessing of version 8.6 data. In this reprocessing, the NOAA-16 SBUV/2 time-dependent calibration is based on the Antarctic snow/ice radiance approach described in DeLand et al. (2012), due to problems with the behavior of the onboard calibration system previously used to characterize that instrument (M. T. DeLand, personal communication, 2013). This procedure was previously developed and used for the NOAA-17 and NOAA-18 calibration in the v8.6 data. The NOAA-17 overpass times fell between 9:36 and 10:36 LST between 2002 and 2009, and the afternoon overpass times of NOAA-16 and NOAA-18 fell between 13:36 and 14:36 LST for a year or more during those years. The NOAA-17 minus NOAA-18 profile (red) and the NOAA-17 minus NOAA-16

profile (blue) are compared in the figure with the MWR profile (black, selected data) for 9:36 to 10:36 LST minus its profile for 13:36 to 14:36 LST. The shapes of these profiles are very similar. Seventy-five percent of the total number of MWR-SBUV/2 differences between pressure-corresponding data points are < 1 %. The exceptions are in the 1 to 2 hPa range. All are < 1.5 %. The points on the average of the two MWR-SBUV/2 profiles are all < 1 %, with a slight positive bias of ~ 0.5 % from ~ 20 to 2 hPa.

In addition to the black profile derived from selected MWR data, Fig. 7 includes a gray profile made from MWR data without limitations on temperature or elevation angle. The differences are < 0.6 % above 24 hPa (~ 26 km). This result suggests that the MWR measurements are less affected by time-dependent systematic errors during the day than during the day-night transition.

3.1 Summary of comparisons

We have calculated profile differences in ozone expressed in normalized units as described in Sect. 2.1 between two times of day at or over MLO from measurements made by MWR, Aura-MLS, UARS-MLS, SMILES, and two pairings of SBUV/2 instruments. These results cover the time periods of afternoon–night, morning–night, and morning–afternoon. The MWR, Aura-MLS, and SMILES afternoon–night profiles shown in Fig. 5 are mutually consistent, each agreeing with any other to within a maximum of 1.5 % and typically within 1.2 % up to 0.6 hPa (~ 52 km). If we take the average of these three profiles to be the best available estimate of the true difference profile over this time interval we find that all individual profiles lie within 1 % of it over the above altitude range. The comparisons between the morning–afternoon profile measured with the MWR and those measured with pairs of SBUV/2 instruments as shown in Fig. 7 are also consistent, with differences of < 1 % from 42 to 0.6 hPa (~ 22 to 52 km). The morning–night comparison using MWR, UARS-MLS, and SMILES, however, is poorer. Above 1 hPa, differences between the SMILES profile and the corresponding MWR profile can reach 2.7 %, and differences between the UARS-MLS profile and its corresponding MWR profile can reach 2.2 %. However, the differences in both cases are typically < 1.7 %.

3.2 Uncertainty in MWR measurements

The only tests we have of any diurnally varying systematic errors that may remain in the MWR measurements come from the character of the errors seen in Fig. 2 and the comparisons discussed in Sect. 3.0. If, for the purpose of discussion, we take the average of the afternoon–night Aura-MLS and SMILES profiles shown in Fig. 5 as a reference, we find that the MWR profile differs from it by $< 1\%$ up to 0.3 hPa (~ 56 km). So, there is no evidence from these comparisons for MWR systematic errors $> 1\%$ during the afternoon–night interval. Likewise, if we take the average of the two SBUV/2 profiles in Fig. 7 as a reference for morning–afternoon differences, we find that the MWR profile differs from it by $< 1\%$ from 42 to 0.6 hPa (~ 22–52 km). However, a similar procedure for the morning–night profiles in Fig. 6 yields a worse result. We computed the difference between the SMILES profile and its corresponding MWR profile in Fig. 6, and for the UARS-MLS profile and its corresponding MWR profile. We take the average of these as the difference between the MWR results and combined SMILES and UARS-MLS results. The absolute values of points on this profile are $< 1.7\%$ up to 0.2 hPa (~ 58 km) and 85 % of them lie within 1.5 %. Alternatively, the morning–night differences can be estimated by combining the afternoon–night comparison using Aura-MLS and SMILES with the morning–afternoon comparison using SBUV/2 data, both of which show differences $< 1\%$. Because this procedure involves the uncertainties in both comparisons, the estimated combined uncertainty is larger than the individual ones by a factor of $2^{0.5}$, assuming that the morning–night and morning–afternoon validation resources are statistically independent. This process yields an uncertainty estimate of 1.4 %. Given this value, and the fact that eighty-five percent of the total number of direct morning–night differences are within 1.5 %, we believe it is reasonable to take 1.5 % as the MWR systematic limit for the morning–night interval.

Title Page

Abstract | Introduction

Conclusions | References

Tables | Figures

◄ | ►I

◄ | ►

Back | Close

Full Screen / Esc

Printer-friendly Version

Interactive Discussion

4   Comparisons of MWR measurements with GEOSCCM models

In Fig. 8 we display measured and model calculated ozone values for each hour of the day at twelve pressure levels. The measured values are based on the selected MLO MWR data, which have been binned hourly and averaged over the months of March in all years from 1996 to 2012 to minimize statistical fluctuations. The model runs were based on conditions for March 2005. Both the measurements and the modeled results have been normalized to their midnight values.

The model results are from two implementations of the Goddard Earth Observing System Chemistry Climate Model (GEOSCCM). GEOSCCM couples dynamics from the Goddard Earth Observing System (GEOS) general circulation model (GCM) with a representation of atmospheric chemical processes. GEOSCCM$_{STRATCHEM}$ uses the stratospheric chemistry package first developed for the Goddard Chemical Transport Model (CTM) (Douglass and Kawa, 1999). GEOSCCM$_{STRATCHEM}$ output was extensively evaluated as part of the Stratospheric Processes And their Role in Climate (SPARC) CCMVal project (SPARC CCMVal, 2010). GEOSCCM$_{STRATCHEM}$ performed well in the photolysis computation and representation of radicals, both of direct relevance to this comparison. The second implementation, GEOSCCM$_{STRATTROP}$, uses the comprehensive stratospheric/tropospheric chemistry package developed within the Global Modeling Initiative (GMI) (Duncan et al., 2007; Strahan et al., 2007; Oman et al., 2011). Both chemical representations are coupled to version 5 of the GEOS GCM (Rienicker et al., 2011). Neither GEOSCCM$_{STRATCHEM}$ nor GEOSCCM$_{STRATTROP}$ includes a full representation of mesospheric processes but the processes controlling ozone in the middle to upper stratosphere are complete and the model diurnal cycle is thought to be realistic at altitudes $\lesssim 52$ km (0.5 hPa).

The MWR vertical resolution is poorer than that of the models, which have 1 km level spacing. We convolved the model output with the microwave averaging kernels to minimize resolution effects on the MWR-model comparison. Above 0.5 hPa we truncated the model output and spliced on a reasonable profile, namely the MWR a priori

profile for March, over the pressure range 0.5 to 0.01 hPa before performing the convolution. We note that the resolution effects would be small even if the model output was compared directly with the MWR measurements. To test this, we compared the GEOSCCM$_{STRATCHEM}$ model output vs. time of day at twelve pressure levels between 56 and 0.1 hPa to its output after it had been treated by the above procedure. Between 32 and 2.4 hPa ($\sim$ 24 to 41 km) the direct and convolved model outputs differ by < 0.6 %. The largest difference is 1.5 % at 1.3 hPa ($\sim$ 46 km). Thus errors introduced by convolving the spliced model and a priori profiles are negligible.

Returning to Fig. 8, we see that the models and MWR measurements agree well, mostly within the $\sim$ 1 % (2σ) estimated statistical errors. There are several interesting features. Most notable is the different evolution of the ozone in the pre-dawn and morning hours in the four layers from 3.2 hPa to 1.3 hPa. At these layers the morning MWR data can be 1.5 to 2 % higher than the model values. In the hours just before dawn the observed ozone increases while the model output stays near zero until just after sunrise. The observed values generally remain higher than the model output through the morning hours. In the comparisons shown in Fig. 6, the morning–night differences from the MWR fell at or between those from UARS-MLS and SMILES. Similarly, in Fig. 7, the morning–afternoon MWR differences fell between the NOAA-17 minus NOAA-16 SBUV/2 and NOAA-17 minus NOAA-18 SBUV/2 differences. Although the scatter between results in each of these cases is larger than those displayed in Fig. 5, the MWR results are not outliers. These two cases, especially when taken together, do not support a systematic MWR measurement error of the order of 2 % in the 3.2 to 1.8 hPa range. We also have inspected difference spectra for the month of March, similar to those shown in Fig. 3, and have found that they are qualitatively consistent with the pre-dawn increase described above. We note that the comparisons described in Sect. 3 do not directly cover the pre-dawn time period. However, we are not aware of any unresolved issues that would affect the measurements during this period.

There are other instances where the absolute differences between the models and the MWR measurements are approximately equal to or slightly exceed the estimated

statistical errors but these differences should be viewed with caution. Figure 8 shows that both models have slight dips beginning at 7 h at 1.8 hPa and shifting later in time and broadening with decreasing altitude, ending at 9 h at 10 hPa. The measurements show corresponding local minima which are mostly not significant, but between 5.6 and 10 hPa the measurements lie below the GEOSCCM$_{STRATTROP}$ model by $\sim 1\%$. The MWR-SBUV/2 comparison shown in Fig. 7 supports this result; the differences between the MWR and the two NOAA profiles are $< 0.5\%$ in that region. However, the MWR, SMILES, and UARS-MLS profiles in Fig. 6 are not very consistent there. So, these MWR-model discrepancies are not large enough to be considered significant when the mixed comparison results discussed in Sect. 3.1 are taken into account. The same is true for the declining measured ozone values seen during the day at 18 hPa and below.

5 Conclusions

We have searched for diurnally varying systematic effects in the data produced by the NDACC microwave ozone profiling instrument (MWR) at Mauna Loa, Hawaii by inspecting differences between spectra taken at different times of day (e.g. afternoon–night). We established criteria for signal beam elevation angle and diurnal building temperature variations that minimize systematic artifacts in these spectra and hence their effects on the retrieved profiles. We selected data according to these criteria and used them in intercomparisons of diurnal difference profiles between three instrument types: the MWR, satellite-borne microwave limb sounders (UARS-MLS, Aura-MLS, and SMILES), and solar backscattered ultraviolet instruments (SBUV/2 on NOAA-16, 17, and 18). We considered three pairs of times. For afternoon–night, the consensus between MWR, Aura-MLS, and SMILES is very good, with maximum profile differences between any pair of these $< 1.5\%$ up to 0.6 hPa (~ 52 km), and differences between any one and the average of the three $< 1\%$. The consensus is equally good for the MWR-SBUV/2 afternoon-morning comparisons. However, it is poorer for the MWR,

UARS-MLS, and SMILES morning–night comparisons, with 85 % of the differences between pairs < 1.5 % and the remaining up to 1.7 %. We then compared hourly binned averages of the selected MWR data for the months of March from 1996 to 2012 with output from the NASA-Goddard GEOSCCM model for the month of March 2005. We found that the features seen in the measurements and model output mostly agree to better than 1 to 1.5 % statistical errors at the 2σ level. There is one discrepancy worth noting. The MWR morning–night values are 2 to 3 % higher than the modeled ones from 3.2 to 1.8 hPa (~ 39 to 43 km), and the measured values are increasing compared to the modeled values before sunrise in this region. The anomalies are statistically significant just before sunrise from 2.4 to 1.3 hPa. The intercomparisons give no indication that the MWR values are overestimated in this range, but they do not directly confirm the pre-sunrise increase.

These results suggest that the GEOSCCM model has value for estimating adjustments to be applied when combining measurements of two or more satellite instruments to minimize the effects of real diurnal ozone variations on the consolidated set, or to adjust data of satellite instruments that are in drifting orbits. The good agreement between MWR, Aura-MLS, UARS-MLS, and SMILES suggests that the last three, together with the model, can be used to estimate such adjustments over a wider range of latitudes.

Title Page

Abstract Introduction

Conclusions References

Tables Figures

|◄ ►|

◄ ►

Back Close

Full Screen / Esc

Printer-friendly Version

Interactive Discussion

References

Barath, F. T., Chavez, M. C., Cofield, R. E., Flower, D. A., Frerking, M. A., Gram, M. B., Harris, W. M., Holden, J. R., Jarnot, R. F., Kloezeman, W. G., Klose, G. J., Lau, G. K., Loo, M. S., Maddison, B. J., Mattauch, R. J., McKinney, R. P., Peckham, G. E., Pickett, H. M., Siebes, G., Soltis, F. S., Suttie, R. A., Tarsala, J. A., Waters, J. W., and Wilson, W. J.: The Upper Atmosphere Research Satellite microwave limb sounder instrument, J. Geophys. Res., 98, 10751–10762, 1993.

Chapman, S.: A theory of upper stratospheric ozone, Mem. R. Meteorol. Soc., 3, 103–125, 1930.

Connor, B. J., Siskind, D. E., Tsou, J. J., Parrish, A., and Remsburg, E. E.: Ground based microwave observations of ozone in the upper stratosphere and mesosphere, J. Geophys. Res., 99, 16757–16770, 1994.

Connor, B. J., Parrish, A., Tsou, J. J., and McCormick, M. P.: Error analysis for the ground-based microwave ozone measurements during STOIC, J. Geophys. Res., 100, 9283–9291, 1995.

DeLand, M. T., Taylor, S. L., Huang, L. K., and Fisher, B. L.: Calibration of the SBUV version 8.6 ozone data product, Atmos. Meas. Tech., 5, 2951–2967, doi:10.5194/amt-5-2951-2012, 2012.

Douglass, A. R. and Kawa, S. R.: Contrast between 1992 and 1997 high-latitude spring Halogen Occultation Experiment observations of lower stratospheric HCl, J. Geophys. Res., 104, 18739–18754, doi:10.1029/1999JD900281, 1999.

Duncan, B. N., Strahan, S. E., Yoshida, Y., Steenrod, S. D., and Livesey, N.: Model study of the cross-tropopause transport of biomass burning pollution, Atmos. Chem. Phys., 7, 3713–3736, doi:10.5194/acp-7-3713-2007, 2007.

Farman, J. C., Gardiner, B. G., and Shankin, J. D.: Large losses of total ozone in Antarctica reveal seasonal ClO_x/NO_x interaction, Nature, 315, 207–210, 1985.

Measurement validation and GEOSCCM model comparison

A. Parrish et al.

Title Page

Abstract	Introduction
Conclusions	References
Tables	Figures

Back | Close

Full Screen / Esc

Printer-friendly Version

Interactive Discussion

Frederick, J. E., Cebula, R. P., and Heath, D. F.: Instrument characterization for the detection of long term changes in stratospheric ozone: an analysis of the SBUV/2 radiometer, J. Atmos. Ocean. Tech., 3, 272–480, 1986.

Froidevaux, L., Read, W. G., Lungu, T. A., Cofield, R. E., Fishbein, E. F., Flower, D. A., Jarnot, R. F., Ridenoure, B. P., Shippony, Z., Waters, J. W., Margitan, J. J., McDermid, I. S., Stachnik, R. A., Peckham, G. E., Braathen, G., Deshler, T., Fishman, J., Hofmann, D. J., and Oltmans, S. J.: Validation of UARS Microwave Limb Sounder ozone measurements, J. Geophys. Res., 101, 10017–10060, doi:10.1029/95JD02325, 1996.

Froidevaux, L., Jiang, Y. B., Lambert, A., Livesey, N. J., Read, W. G., Waters, J. W., Browell, E. V., Hair, J. W., Avery, M. A., McGee, T. J., Twigg, L. W., Sumnicht, G. K., Jucks, K. W., Margitan, J. J., Sen, B., Stachnik, R. A., Toon, G. C., Bernath, P. F., Boone, C. D., Walker, K. A., Filipiak, M. J., Harwood, R. S., Fuller, R. A., Manney, G. L., Schwartz, M. J., Daffer, W. H., Drouin, B. J., Cofield, R. E., Cuddy, D. T., Jarnot, R. F., Knosp, B. W., Perun, V. S., Snyder, W. V., Stek, P. C., Thurstans, R. P., and Wagner, P. A.: Validation of Aura Microwave Limb Sounder stratospheric ozone measurements, J. Geophys. Res., 113, D15S20, doi:10.1029/2007JD008771, 2008.

Haefele, A., Hocke, K., Kämpfer, N., Keckhut, P., Marchand, M., Bekki, S., Morel, B., Egorova, T., and Rozanov, E., Diurnal changes in middle atmospheric H_2O and O_3: observations in the Alpine region and climate models, J. Geophys. Res., 113, D17303, doi:10.1029/2008JD009892, 2008.

Huang, F. T., Reber, C. A., and Austin, J.: Ozone diurnal variations observed by UARS and their model simulation, J. Geophys. Res., 102, 12971–12985, doi:10.1029/97JD00461, 1997.

Huang, F. T., Mayr, H. G., Russell III, J. M., and Mlynczak, M. G.: Ozone diurnal variations in the stratosphere and lower mesosphere, based on measurements from SABER on TIMED, J. Geophys. Res., 115, D24308, doi:10.1029/2010JD014484, 2010.

Imai, K., Manago, N., Mitsuda, C., Naito, Y., Nishimoto, E., Sakazaki, T., Fujiwara, M., Froidevaux, L., von Clarmann, T., Stiller, G. P., Murtagh, D. P., Rong, P.-P., Mlynczak, M. G., Walker, K. A., Kinnison, D. E., Akiyoshi, H., Nakamura, T., Miyasaka, T., Nishibori, T., Mizobuchi, S., Kikuchi, K.-I., Ozeki, H., Takahashi, C., Hayashi, H., Sano, T., Suzuki, M., Takayanagi, M., and Shiotani, M.: Validation of ozone data from the superconducting Submillimeter-Wave Limb-Emission Sounder (SMILES), J. Geophys. Res., 118, 5750–5769, doi:10.1002/jgrd.50434, 2013.

Title Page

Abstract | Introduction

Conclusions | References

Tables | Figures

◄ | ►

◄ | ►

Back | Close

Full Screen / Esc

Printer-friendly Version

Interactive Discussion

JAXA, Level 2 product v2.1 (007-08-0310) release notes, SMILES office, Japan Aerospace Exploration Agency, Saitama, Japan, available at: http://smiles.isas.jaxa.jp/access/SMILES_L2_product_v2-1_release_note.pdf (last access: December 2013), 2012.

Kikuchi, K., Nishibori, T., Ochiai, S., Ozeki, H., Irimajiri, Y., Kasai, Y., Koike, M., Manabe, T., Mizukoshi, K., Murayama, Y., Nagahama, T., Sano, T., Sato, R., Seta, M., Takahashi, C., Takayanagi, M., Masuko, H., Inatani, J., Suzuki, M., and Shiotani, M.: Overview and early results of the superconducting Submillimeter-Wave Limb-Emission Sounder (SMILES), J. Geophys. Res., 115, D23306, doi:10.1029/2010JD014379, 2010.

Livesey, N. J., Read, W. G., Froidevaux, L., Waters, J. W., Santee, M. L., Pumphrey, H. C., Wu, D. L., Shippony, Z., and Jarnot, R. F.: The UARS Microwave Limb Sounder version 5 data set: theory, characterization, and validation, J. Geophys. Res., 108, 4378, doi:10.1029/2002JD002273, 2003.

Livesey, N. J., Read, W. G., Froidevaux, L., Lambert, A., Manney, G. L., Pumphrey, H. C., Santee, M. L., Schwartz, M. J., Wang, S., Cofield, R. E., Cuddy, D. T., Fuller, R. A., Jarnot, R. F., Jiang, J. H., Knosp, B. W., Stek, P. C., Wagner, P. A., and Wu, D. L.: Version 3.3 Level 2 data quality and description document, Version 3.3x-1.0, Jet Propulsion Laboratory, Pasadena, California, available at: http://mls.jpl.nasa.gov/data/v3-3_data_quality_document.pdf (last access: December 2013), 2011.

Oman, L. D., Ziemke, J. R., Douglass, A. R., Waugh, D. W., Lang, C. Rodriguez, J. M., and Nielsen, J. E.: The response of tropical tropospheric ozone to ENSO, Geophys. Res. Lett., 38, L13706, doi:10.1029/2011GL047865, 2011.

Parrish, A.: Millimeter-wave remote sensing of ozone and trace constituents in the stratosphere, Proc. IEEE, 82, 1915–1929, 1994.

Parrish, A., deZafra, R. L., Solomon, P. M., and Barrett, J. W.: A ground-based technique for millimeter wave spectroscopic observations of stratospheric trace constituents, Radio Science, 23, 106–118, 1988.

Parrish, A., Connor, B. J., Tsou, J. J., McDermid, I. S., and Chu, W. P.: Ground-based microwave monitoring of stratospheric ozone, J. Geophys. Res., 97, 2541–2546, 1992.

Rodgers, C. D.: Retrieval of atmospheric temperature and composition from remote measurements of thermal radiation, Rev. Geophys., 14, 609–624, 1976.

Rienecker, M., Suarez, M. J., Gelaro, R., Todling, R., Bacmeister, J., Liu, E., Bosilovich, M. G., Schubert, S. D., Takacs, L., Kim, G.-K., Bloom, S., Chen, J., Collins, D., Conaty, A., da Silva, A., Gu, W., Joiner, J., Koster, R. D., Lucchesi, R., Molod, A., Owens, T., Pawson, S., Pegion,

Title Page

Abstract | Introduction

Conclusions | References

Tables | Figures

◀ | ▶

◁ | ▷

Back | Close

Full Screen / Esc

Printer-friendly Version

Interactive Discussion

P., Redder, C. R., Reichle, R., Robertson, F. R., Ruddick, A. G., Sienkiewicz, M., and Woollen, J.: MERRA: NASA's Modern-Era Retrospective Analysis for Research and Applications, J. Climate, 24, 3624–3648, doi:10.1175/JCLI-D-11-00015.1, 2011.

Rowland, F. J. and Molina, M. J.: Chloroflouromethanes in the environment, Rev. Geophys., 13, 1–35, 1975.

Sakazaki, T., Fujiwara, M., Mitsuda, C., Imai, K., Manago, N., Naito, Y., Nakamura, T., Akiyoshi, H., Kinnison, D., Sano, T., Suzuki, M., and Shiotani, M.: Diurnal ozone variations in the stratosphere revealed in observations from the Superconducting Submillimeter-Wave Limb-Emission Sounder (SMILES) on board the International Space Station (ISS), J. Geophys. Res. Atmos., 118, 2991–3006, doi:10.1002/jgrd.50220, 2013.

SPARC: Assessment of Trends in the Vertical Distribution of Ozone, edited by: Harris, N., Hudson, R., and Phillips, C., SPARC report No. 1, Global Ozone Research and Monitoring Project – Report No. 43, Geneva, 1998.

SPARC: Chemistry Climate Model Validation, edited by: Eyring, V., Shepherd, T. G., and Waugh, D. W., SPARC Report No. 5, Global Ozone Research and Monitoring Project – Report No. 43, Geneva, 2010.

Strahan, S. E., Duncan, B. N., and Hoor, P.: Observationally derived transport diagnostics for the lowermost stratosphere and their application to the GMI chemistry and transport model, Atmos. Chem. Phys., 7, 2435–2445, doi:10.5194/acp-7-2435-2007, 2007.

UNEP: Handbook for the Montreal Protocol on substances that deplete the ozone layer, United Nations Environment Program, Ozone Secretariat, Nairobi, 2006.

Waters, J. W., Froidevaux, L., Harwood, R. S., Jarnot, R. F., Pickett, H. M., Read, W. G., Siegel, P. H., Cofield, R. E., Filipiak, M. J., Flower, D. A., Holden, J. R., Lau, G. K., Livesey, N. J., Manney, G. L., Pumphrey, H. C., Santee, M. L., Wu, D. L., Cuddy, D. T., Lay, R. R., Loo, M. S., Perun, V. S., Schwartz, M. J., Stek, P. C., Thurstans, R. P., Boyles, M. A., Chandra, K. M., Chavez, M. C., Gun-Shing, C., Chudasama, B. V., Dodge, R., Fuller, R. A., Girard, M. A., Jiang, J. H., Yibo, J., Knosp, B. W., LaBelle, R. C., Lam, J. C., Lee, K. A., Miller, D., Oswald, J. E., Patel, N. C., Pukala, D. M., Quintero, O., Scaff, D. M., Van Snyder, W., Tope, M. C., Wagner, P. A., and Walch, M. J.: The Earth Observing System Microwave Limb Sounder (EOS MLS) on the Aura satellite, IEEE T. Geosci. Remote., 44, 1075–1092, doi:10.1109/TGRS.2006.873771, 2006.

WMO (World Meteorological Organization): Scientific assessment of ozone depletion: 2010, Global Ozone Research and Monitoring Project – Report No. 52, Geneva, 2011.
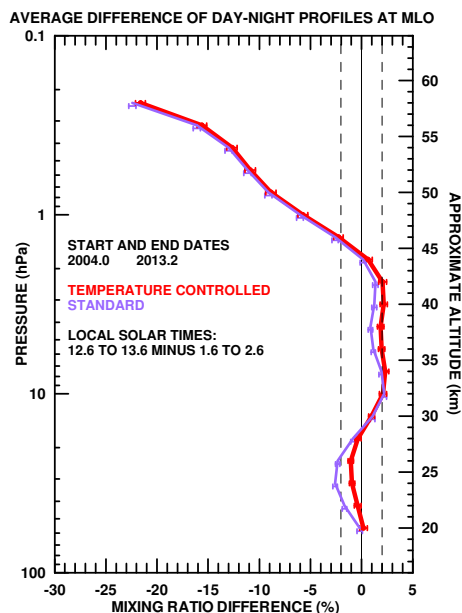
Fig. 1. MWR measurements of daytime (12:36 to 13:36 LST) minus nighttime (01:36 to 02:36 LST) ozone differences at Mauna Loa from data recorded within 1.2 °C of the room thermostat setting (red) and standard data without this restriction (violet), as described in the text. Individual measurements were averaged over the period January 2004 to March 2013 and combined and normalized as described in Sect. 2.1 to make this figure. The error bars are set equal to $2 \times \text{rms} \times n^{-0.5}$, where n is the number of individual measurements in the average for each data point and rms is the root-mean-square of the individual values in that set of measurements. The vertical positions of the error bars have been offset slightly from their nominal pressure values to display the errors more clearly. Vertical dotted lines at ±2 % are provided as a guide to the eye.

Title Page

Abstract | Introduction

Conclusions | References

Tables | Figures

◄ | ►►

◄ | ►

Back | Close

Full Screen / Esc

Printer-friendly Version

Interactive Discussion
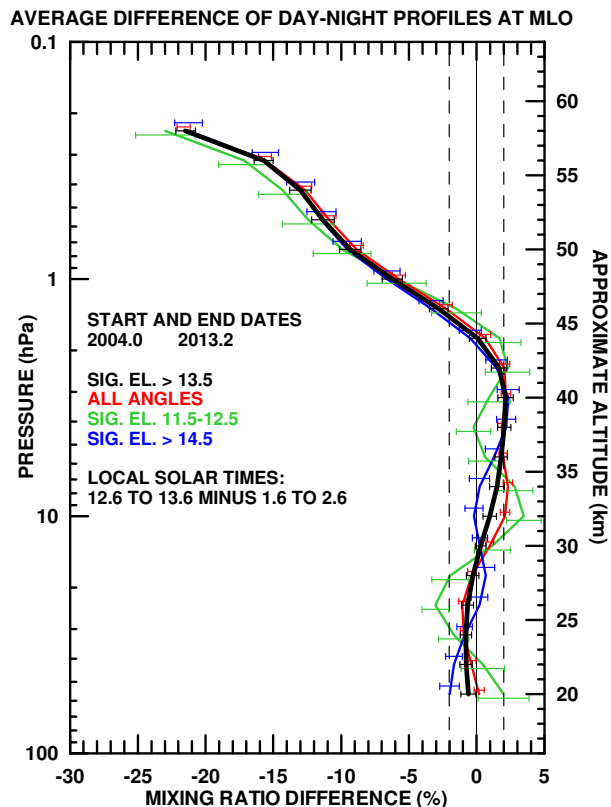
Fig. 2. Day-night difference profiles derived from data that were recorded when the room temperature was well controlled and the signal beam elevation angle was within specified limits, as follows: black; selected data, as used for this work, with elevation angle > 13.5°; red, no angle limits, corresponding to the red profile in Fig. 1; green, 11.5 to 12.5°; blue, > 14.5°. Errors and other details are as desscribed in the caption for Fig. 1. See text for discussion of the profiles.

Title Page

Abstract | Introduction

Conclusions | References

Tables | Figures

|◄ | ►|

◄ | ►

Back | Close

Full Screen / Esc

Printer-friendly Version

Interactive Discussion
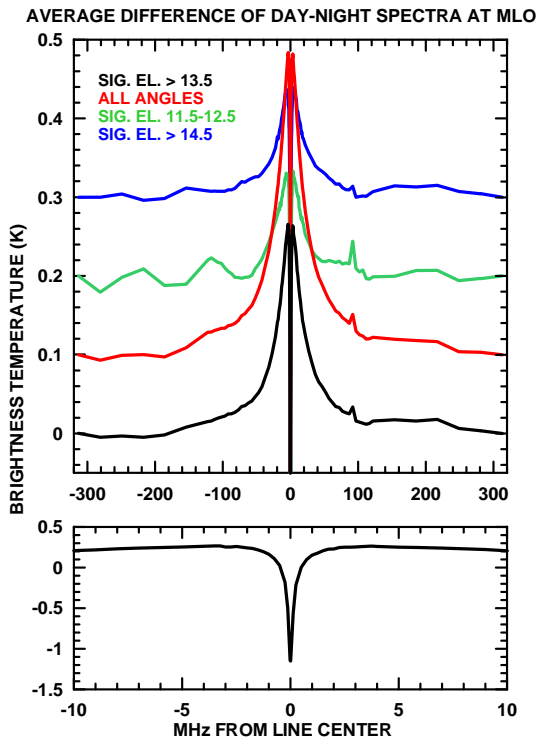
Fig. 3. The top panel displays difference spectra corresponding to the difference profiles shown in Fig. 2. The nighttime reference spectrum is subtracted from the daytime spectrum in each case. The abscissa is expressed in units of brightness temperature in degrees Kelvin. The ordinate is expressed as an offset from the ozone line center frequency (110 836.04 MHz). The elevation angle ranges are indicated in the panel. The black spectrum corresponds to the temperature controlled data with elevation angles > 13.5°. Each of the colored spectra has been offset upward by 0.1 K from the one below it for clarity. The bottom panel displays the very narrow negative central feature with an expanded frequency scale and a compressed intensity scale.
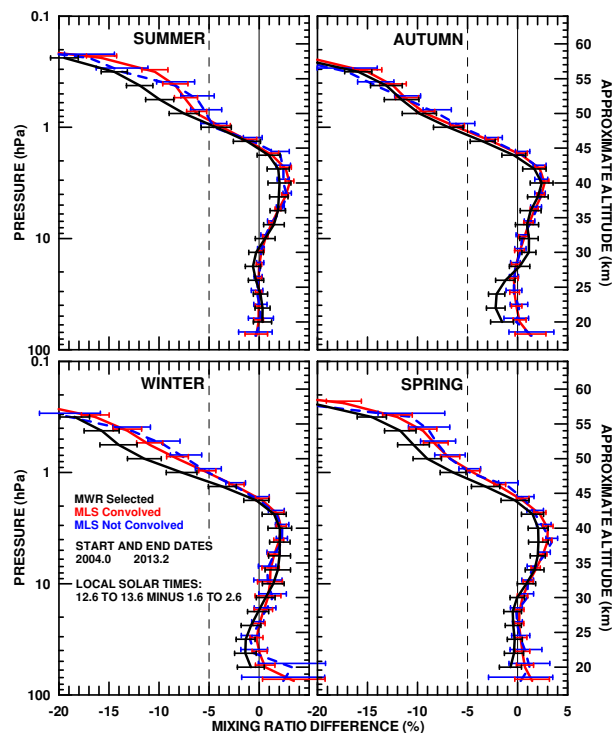
Fig. 4. Day-night ozone differences as measured by Aura-MLS and by the MWR at Mauna Loa. The MWR measurements are shown in black and were derived from selected data as described in Sect. 2. The Aura-MLS measurements shown in red have been convolved with the averaging kernels of the MWR, while those shown as blue dashed lines were derived from the original data. Measurements from each instrument have been averaged over the indicated period. The dates and times associated with the observations, the normalization technique, and the method of calculating the error bars are as described in the caption for Fig. 1. Error bars have been offset from their nominal pressure values for clarity

Title Page

Abstract | Introduction

Conclusions | References

Tables | Figures

◄ | ►

◄ | ►

Back | Close

Full Screen / Esc

Printer-friendly Version

Interactive Discussion
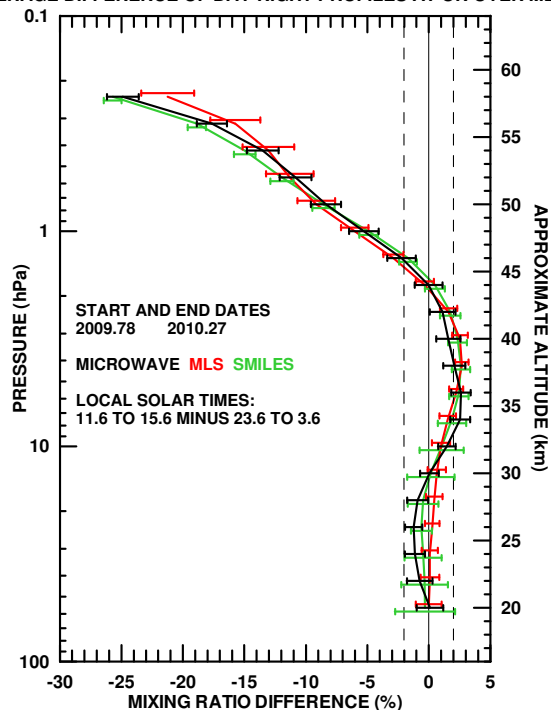
Fig. 5. Afternoon–night differences derived from SMILES (green), Aura-MLS (red), and MWR selected data (black) at Mauna Loa. The SMILES and Aura-MLS measurements have been convolved with the MWR averaging kernels. All measurements have been averaged over the indicated SMILES observing period. The afternoon SMILES and MWR measurement pairs were averaged over the periods 11:36 to 15:36 and the nighttime over 23:36 to 03:36 LST. The time ranges for MLS are narrower, 13:00 to 13:48 LST and 01:30 to 02:24 LST because Aura is in a sun-synchronous orbit. Individual measurements were averaged over the period 12 October 2009 to 9 April 2010 and combined as described in Sect. 2.1 to make these profiles. Error bars are calculated and displayed as described in the caption for Fig. 1.

Full Screen / Esc

Printer-friendly Version

Interactive Discussion
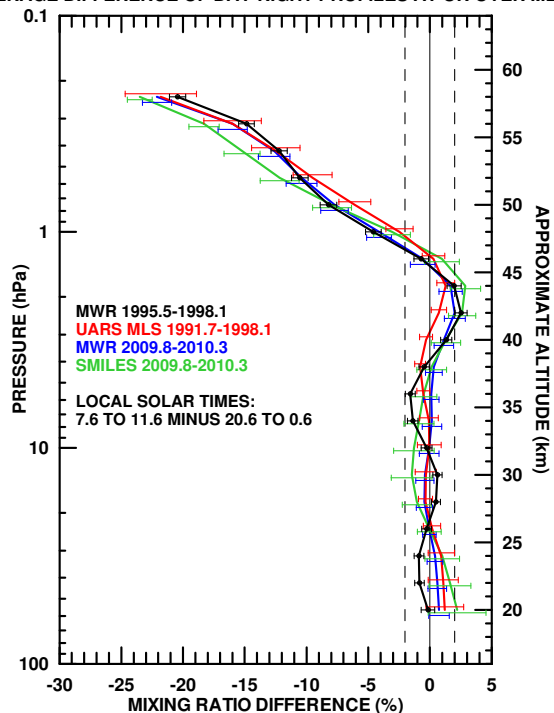
Fig. 6. Average differences between morning (07:36 to 10:36 LST) and nighttime reference (21:36 to 00:36 LST) from UARS-MLS, SMILES, and MWR data. The data were normalized as described in Sect. 2.1. The SMILES profile shown in green and MWR profile shown in blue were averaged over the period 12 October 2009 to 20 April 2010. The MWR profile shown in black was averaged over January 1995 to February 1998; the UARS-MLS profile shown in red over September 1991 to February 1998. The SMILES and UARS-MLS data have been convolved with the MWR averaging kernels. The error bars are calculated and displayed as described in the caption for Fig. 1.

Full Screen / Esc

Printer-friendly Version
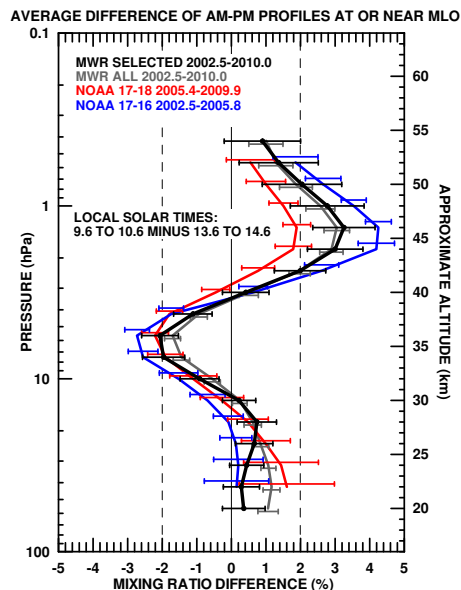
Interactive Discussion

Fig. 7. Percentage differences between morning and afternoon ozone profiles. The morning satellite profiles are all from NOAA-17 SBUV/2 measurements, averaged between 09:36 and 10:36 LST. The reference afternoon profiles are from NOAA-18 (red) or NOAA-16 (blue) and were averaged from 13:36 to 14:36 LST. They were subtracted from the morning profiles and normalized as described in Sect. 2.1. Differences between morning and afternoon (reference) MWR measurements taken during the same time blocks are shown for comparison in black (selected data) or gray (all data). The data used for the NOAA-17 and 16 profile were averaged from July 2002 to December 2005; those for the NOAA-17 and 18 profile were averaged from June 2005 to November 2009. MWR data were averaged from July 2002 to December 2009. Error bars are calculated and displayed as described in the caption for Fig. 1. The SBUV/2 data have not been convolved with the MWR averaging kernels because the resolutions of the two instruments are similar.
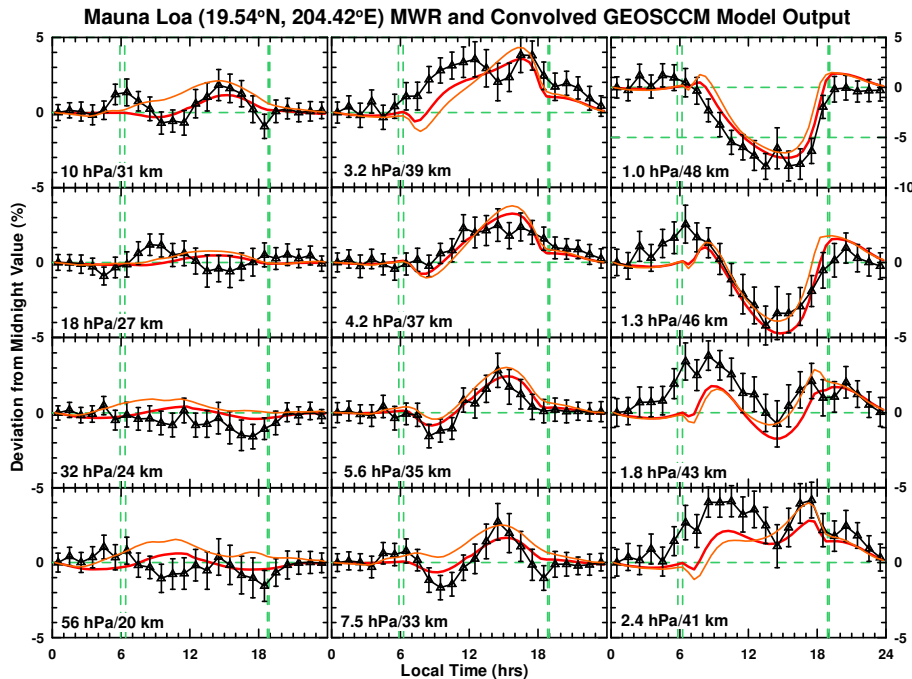
Fig. 8. Measured and modeled ozone values for each hour of the day in March, normalized to the corresponding midnight values. Measured values (black) are derived from selected MWR data, averaged over the months of March from 1996 to 2012, at pressure levels between 56 hPa (bottom left panel) and 1 hPa (top right panel). The scales for the panels from 2.4 to 1 hPa are given on the right hand ordinates; the scales for all others are given on the left hand ordinates. All values have been normalized to the midnight value as described in Sect. 2.1. Two standard deviation statistical error estimates described in the text are shown as error bars. The NASA/GSFC GEOSCCM$_{STRAT\_CHEM}$ (red) and GEOSCCM$_{STRAT\_TROP}$ (orange) model outputs are for March 2005 as described in the text. The model outputs have been convolved with the MWR averaging kernels. Dashed green vertical lines indicate the earliest and latest sunrise and sunset times for March.

Title Page

Abstract · Introduction

Conclusions · References

Tables · Figures

◄ · ►I

◄ · ►

Back · Close

Full Screen / Esc

Printer-friendly Version

Interactive Discussion